A FINITE UNLOADED QUALITY-FACTOR RESONATORS BASED NEGATIVE GROUP DELAY CIRCUIT AND ITS APPLICATION TO DESIGN POWER DIVIDER

Girdhari Chaudhary and Yongchae Jeong
Division of Electronic and Information Engineering, IT Convergence Research Center, Chonbuk National University, Jeonju, Republic of Korea; Corresponding author: ycjeong@jbnu.ac.kr

Received 3 May 2016

ABSTRACT: *This paper presents a novel approach to design a negative group delay (NGD) circuit based on finite unloaded quality-factor resonators. The proposed topology does not require a lumped element resistor to generate NGD. The NGD can be controlled by coupling between source and resonators as well as by unloaded quality-factor of resonators. Similarly, the NGD bandwidth can be controlled by coupling between resonators. The proposed topology can further apply to design power divider. The design theory of the proposed topology is proven through fabrication of NGD circuit and power divider at a center frequency of 2.14 GHz. The measurement results are in good agreement with simulations and predicated theoretical results.* © 2016 Wiley Periodicals, Inc. Microwave Opt Technol Lett 58:2918–2921, 2016; View this article online at wileyonlinelibrary.com. DOI 10.1002/mop.30184

Key words: *coupling matrix; negative group delay; power divider; finite unloaded quality-factor*

1. INTRODUCTION

Understanding effect of group delay (GD) has become critical as the GD influences performance of RF/electronic circuits and systems. The GD can be investigated by examining the phase variation of transmitting scattering parameter. Recently, a negative group delay (NGD) refers to the phenomenon whereby an electromagnetic wave traverses a dispersive material or electronic circuit in such a manner that its amplitude envelope is advanced through media rather than undergoing delay [1]. However, this phenomenon does not violate a causality, since the initial transient of the pulse is still limited to the front velocity that does not exceed the speed of light in a vacuum [1,2].

NGD circuits have used in various practical applications of RF communication systems, such as shortening or reducing delay lines, enhancing the efficiency of feedforward linear amplifiers, designing broadband and constant phase shifters, realization of non-Foster reactive elements, and minimizing beam-squint in series-fed antenna arrays [3–6]. The conventional NGD circuit topologies utilized the resistors along with resonators to generate the NGD and these circuits suffer from high signal attenuation, narrow magnitude flatness, and NGD bandwidth. To overcome these problems, researchers have attempted to design NGD circuits using different methods such as cross-coupling between resonators, increasing the number of resonators, and transversal-filter topologies [7–9]. On the other hand, these works showed very high signal attenuation (>28 dB for −1 ns). Moreover, except for the work of Ref. [9], these NGD circuits also used resistor to generate NGD, which prevents fully distributed circuit realization.

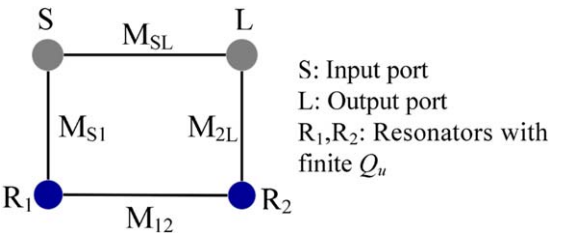

Figure 1 Coupling diagram of the proposed NGD circuit. [Color figure can be viewed at wileyonlinelibrary.com]

Modern RF wireless communication systems require highly linear high power amplifiers because of the complex modulation techniques that are needed to handle the higher data rate transmissions. A predistortion method is cost-effective linearization technique and has the advantages of low power consumption and simple circuit configuration [10]. In this technique, it is crucial to match GDs, the magnitudes, and phases of signals simultaneously in different paths of the predistortion circuit to ensure linearity enhancement. For this purpose, a delay element, attenuator, and phase shifter are used in predistortion circuits. Therefore, a power divider with predefined NGD would be promising for positive GD compensation in the predistortion amplifier that can eliminate the delay element and attenuator.

In this paper, a novel topology of NGD is presented based on finite unloaded quality-factor resonators. The proposed topology does not require any resistor to generate the NGD. Furthermore, this topology can apply to design power divider with predefined NGD characteristics.

2. DESIGN THEORY

2.1. Finite Unloaded Quality-Factor Resonators Based NGD Circuit

Figure 1 shows the coupling diagram of the proposed NGD circuit using finite unloaded quality-factor (Q_u) resonators where both external couplings (M_{S1} and M_{L2}) are equal. Similarly, the self-coupling values (M_{11} and M_{22}), the source-to-load (M_{SL}) coupling, and load-to-source coupling (M_{LS}) have the same magnitude. The (N + 2) × (N + 2) coupling matrix corresponding to the coupling diagram shown in Figure 1 is given as [1].

$$M=\begin{bmatrix} 0 & M_{S1} & 0 & M_{SL} \\ M_{S1} & M_{11} & M_{12} & 0 \\ 0 & M_{12} & M_{22} & M_{S1} \\ M_{SL} & 0 & M_{S1} & 0 \end{bmatrix} \tag{1}$$

where the subscripts S, L, 1, and 2 correspond to the source, load, the first resonator, and the second resonator, respectively.

Assuming lossless source to load coupling coefficient and $M_{11} = M_{22} = -\mathrm{j}/Q_u\Delta$, reflection and transmission coefficients of the proposed NGD circuit can be obtained as (2) by using filter synthesis theory [11].

$$S_{11\_\mathrm{NGD}}=1-\frac{\frac{1}{\Delta^2}\left(\frac{\omega}{\omega_0}-\frac{\omega_0}{\omega}\right)^2-\frac{M_{S1}^2}{Q_u\Delta}-M_{12}^2-\frac{1}{Q_u^2\Delta^2}-j\frac{2}{Q_u\Delta^2}\left(\frac{\omega}{\omega_0}-\frac{\omega_0}{\omega}\right)-j\frac{M_{S1}^2}{\Delta}\left(\frac{\omega}{\omega_0}-\frac{\omega_0}{\omega}\right)}{0.5\left(M_{SL}^2+1\right)\left\{\frac{1}{\Delta^2}\left(\frac{\omega}{\omega_0}-\frac{\omega_0}{\omega}\right)^2-\frac{1}{Q_u^2\Delta^2}-M_{12}^2\right\}+M_{12}M_{S1}^2M_{SL}-0.5M_{S1}^4-\frac{M_{S1}^2}{Q_u\Delta}-j\frac{1}{\Delta}\left(\frac{\omega}{\omega_0}-\frac{\omega_0}{\omega}\right)\left(M_{S1}^2+\frac{1}{Q_u\Delta}+\frac{M_{SL}^2}{Q_u\Delta}\right)} \tag{2a}$$

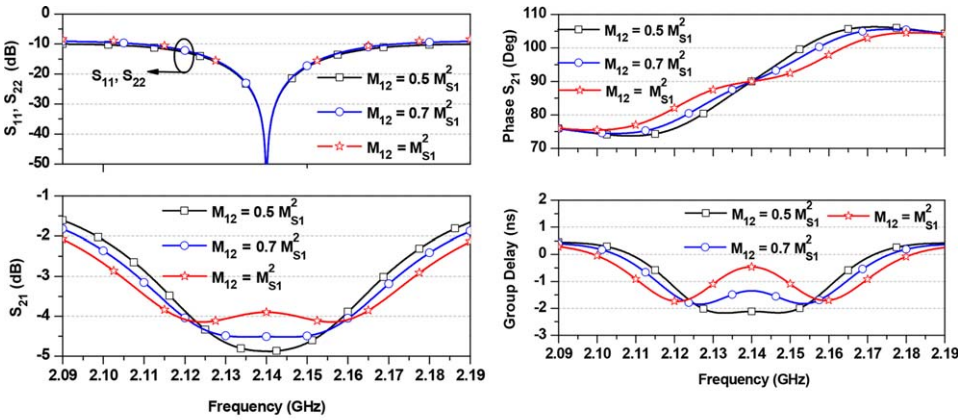

Figure 2 Calculated frequency responses of NGD circuit: (a) *S*-parameter magnitudes and (b) phase/GD characteristics. [Color figure can be viewed at wileyonlinelibrary.com]

$$S_{21\_NGD}=\frac{2\left\{\frac{M_{SL}}{\Delta^2}\left(\frac{\omega}{\omega_0}-\frac{\omega_0}{\omega}\right)^2-M_{SL}M_{12}^2+M_{12}M_{S1}^2-\frac{M_{SL}}{Q_u^2\Delta^2}-j\frac{2M_{SL}}{Q_u\Delta^2}\left(\frac{\omega}{\omega_0}-\frac{\omega_0}{\omega}\right)\right\}}{\left(2M_{S1}^2+\frac{2M_{SL}^2}{Q_u\Delta}+\frac{2}{Q_u\Delta}\right)\frac{1}{\Delta}\left(\frac{\omega}{\omega_0}-\frac{\omega_0}{\omega}\right)+j\left(M_{SL}^2+1\right)\left\{\frac{1}{\Delta^2}\left(\frac{\omega}{\omega_0}-\frac{\omega_0}{\omega}\right)^2-\frac{1}{Q_u^2\Delta^2}-M_{12}^2\right\}-j\frac{2M_{S1}^2}{Q_u\Delta}+2jM_{12}M_{S1}^2M_{SL}-jM_{S1}^4} \tag{2b}$$

where Δ, ω, and ω_0 are 3-dB fractional bandwidth, operating frequency, and center frequency, respectively. Furthermore, the GD of the proposed circuit can be obtained using [3].

$$\tau_{g\_NGD}=-\frac{d\angle S_{21\_NGD}}{d\omega}=-\frac{d}{d\omega}\left(\tan^{-1}\frac{\mathrm{Im}\,(S_{21})}{\mathrm{Re}\,(S_{21})}\right) \tag{3}$$

where $\mathrm{Im}(S_{21})$ and $\mathrm{Re}(S_{21})$ are the imaginary and real parts of the transmission coefficient (S_{21}), respectively.

For matched input/output ports, S_{11_NGD} in (2a) is set to zero at $\omega=\omega_0$ to find the relationship between M_{SL} and M_{S1} with the assumption of $M_{12}=aM_{S1}^2$, where a is any real positive value. For an arbitrary value of M_{S1}, the relationship between M_{SL} and M_{S1} for matched input/output ports at ω_0 can be found with [4], where positive sign for $M_{S1}>1$ and negative sign for $M_{S1}<1$.

$$M_{SL}=\frac{aM_{S1}^4\mp\sqrt{a^2M_{S1}^8+\left(a^2M_{S1}^4+\frac{1}{Q_u^2\Delta^2}\right)\left\{M_{S1}^4(a^2-1)+\frac{1}{Q_u^2\Delta^2}\right\}}}{a^2M_{S1}^4+\frac{1}{Q_u^2\Delta^2}} \tag{4}$$

To illustrate the above design equations, the calculated responses of the proposed NGD circuit are shown in Figure 2 for different values of the coupling matrix. As observed from Figure 2(a), the input/output output ports are matched at ω_0. Similarly, S_{21} is increased as M_{12} increases toward a higher value. Moreover, the maximum GD at ω_0 and the NGD bandwidth (which is defined as bandwidth when $\mathrm{GD}<0$) are also increased when M_{12} is changed from 0.2738 to 0.5476 as shown in Figure 2(b) implying the need for controlling the coupling between resonators 1 and 2. Therefore, a strong coupling is required for a wider NGD bandwidth. However, this decreases the maximum NGD at ω_0. Therefore, a trade-off occurs between the insertion loss, maximum NGD, and NGD bandwidth.

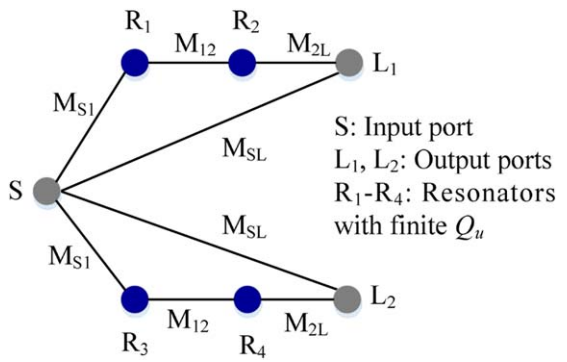

Figure 3 Coupling diagram of the proposed power divider. [Color figure can be viewed at wileyonlinelibrary.com]

2.2. *Application of NGD Circuit to Design Power Divider*

The proposed NGD topology can be applied to design of a power divider. The topology of the proposed power divider is shown in Figure 3, where R_1–R_4 represent four resonators with finite

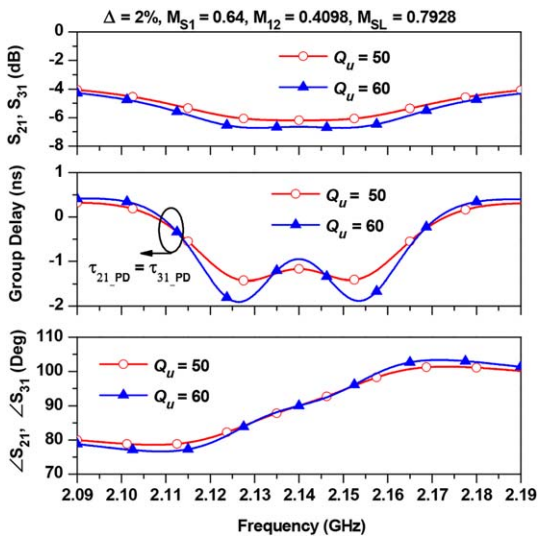

Figure 4 Calculated frequency responses of the proposed power divider with different values of Q_u. [Color figure can be viewed at wileyonlinelibrary.com]

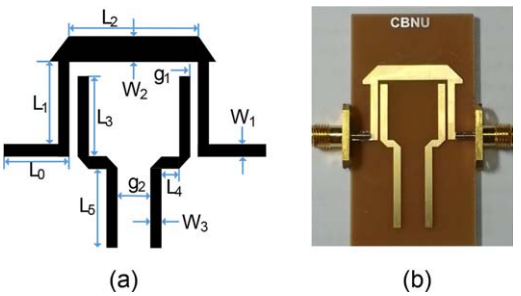

Figure 5 Implemented NGD circuit: (a) EM simulation layout and (b) photograph of fabricated circuit. Physical dimensions: $L_0 = 6.8$, $L_1 = 12.3$, $L_2 = 17.4$, $L_3 = 14.1$, $L_4 = 1.5$, $L_5 = 19.9$, $W_1 = 1.8$, $W_2 = 3.8$, $g_1 = 0.6$, $g_2 = 6$. (Unit: mm). [Color figure can be viewed at wileyonlinelibrary.com]

Q_u and S, L_1, and L_2 denote three ports. Since the structure is symmetrical, even- and odd-mode analysis can be applied to find the S-parameters [12], which is expressed as (5).

$$[S_{PD}] = \begin{bmatrix} S_{11e} & \frac{S_{21e}}{\sqrt{2}} & \frac{S_{21e}}{\sqrt{2}} \\ \frac{S_{21e}}{\sqrt{2}} & \frac{S_{22e}+S_{22o}}{2} & \frac{S_{22e}-S_{22o}}{2} \\ \frac{S_{21e}}{\sqrt{2}} & \frac{S_{22e}-S_{22o}}{2} & \frac{S_{22e}+S_{22o}}{2} \end{bmatrix} \quad (5)$$

where S_{11e}, S_{22e}, S_{21e}, and S_{22o} are S-parameters of even- and odd-mode equivalent sub-circuits, respectively.

Under even-mode excitation, the equivalent circuit is similar to NGD topology shown in Figure 1. Therefore, the transmission coefficients and GDs of power divider can be found as [6].

$$S_{21\_PD} = S_{31\_PD} = \frac{S_{21e}}{\sqrt{2}} = \frac{S_{21\_NGD}}{\sqrt{2}} \quad (6a)$$

$$\tau_{21\_PD} = \tau_{31\_PD} = -\frac{d\angle S_{21\_PD}}{d\omega} = -\frac{d\angle S_{31\_PD}}{d\omega} \quad (6b)$$

Based on above design equations, the calculated frequency responses of the power divider are shown in Figure 4. As observed from this figure, the magnitude as well as NGD is controlled by Q_u of resonators as shown in Figure 4. When the value of Q_u increases from 50 to 60, magnitudes of S_{21} (insertion loss) and NGD are also increased. However, the low value Q_u is preferable for a low insertion loss.

3. EXPERIMENTAL VERIFICATION

The goal of NGD circuit was to achieve a GD of -1 ns and insertion loss of less than 3.8 dB at center frequency (f_0) of 2.14 GHz under the assumption of termination port impedance Z_0 of 50 Ω. The calculated coupling matrix for the given specification of NGD circuit are given as $M_{S1} = 0.69$, $M_{12} = 0.3468$, $M_{SL} = -0.7677$, $Q_u = 50$, and $\Delta = 2\%$.

The resonators are implemented with an open-circuited $\lambda/2$ transmission line. Using HFSS Eigen-mode simulation, Q_u of the $\lambda/2$ resonator in the FR-4 epoxy substrate is estimated to be around 50. Similarly, the coupling between the source and load is implemented with a step-impedance $3\lambda/4$ line. The EM layout and photograph of the fabricated NGD circuit are shown in Figure 5 with physical dimensions. The coupling coefficients between source/load and resonators R_1/R_2 are controlled by varying L_3 and g_1. Similarly, the inter-resonator coupling coefficient is controlled by changing L_5 and g_2.

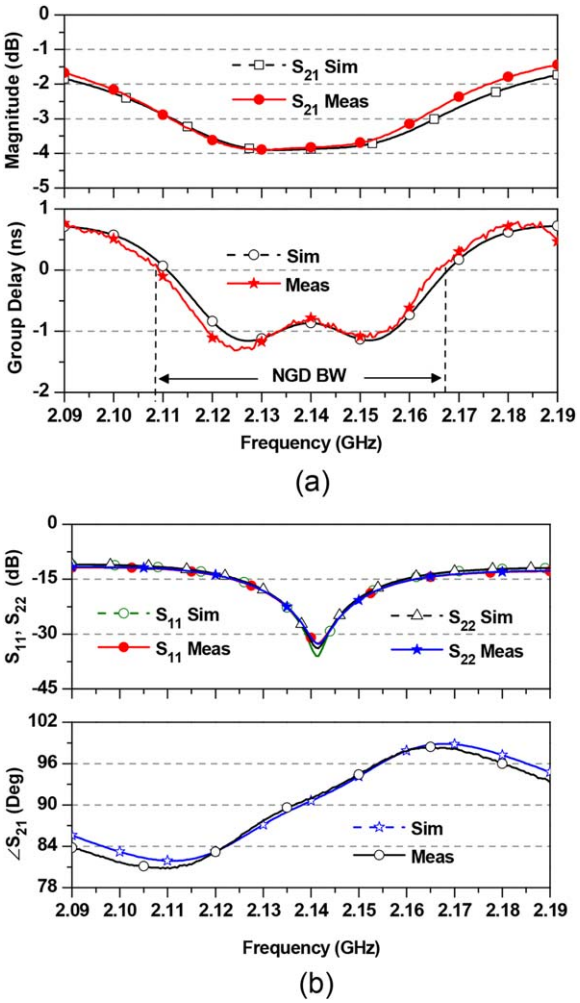

Figure 6 Simulation and measured results of NGD circuit: (a) magnitude/GD and (b) return loss/phase characteristics. [Color figure can be viewed at wileyonlinelibrary.com]

The simulated and measured results of NGD circuit are shown in Figure 6. The measurement results are in good agreement with the simulations. From the measurement results, the insertion loss and GD of S_{21} at $f_0 = 2.14$ GHz are determined as 3.82 dB and -1.031 ± 0.24 ns, respectively. The NGD bandwidth is determined as 60 MHz, providing the NGD-bandwidth product of 0.062. Similarly, the measured return losses (S_{11} and S_{22}) and phase at f_0 are obtained as 30.48 dB and 90.96°, respectively. Moreover, the return loss is higher than 12 dB in the frequency range of 100 MHz.

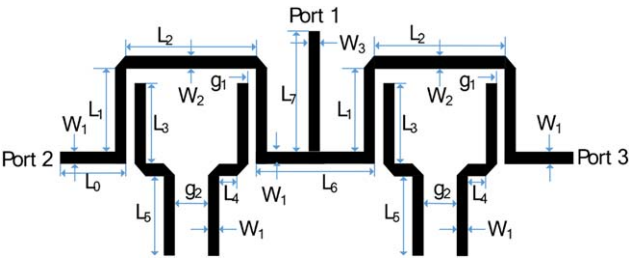

Figure 7 EM simulation layout of power divider with physical dimensions: $W_1 = 1.8$, $W_2 = 3.7$, $W_3 = 2.7$, $L_0 = 8.2$, $L_1 = 12.3$, $L_2 = 17.4$, $L_3 = 14.1$, $L_4 = 1.5$, $L_5 = 20$, $L_6 = 19.1$, $L_7 = 20.2$, $g_1 = 0.6$, $g_2 = 6$. (Unit: mm). [Color figure can be viewed at wileyonlinelibrary.com]

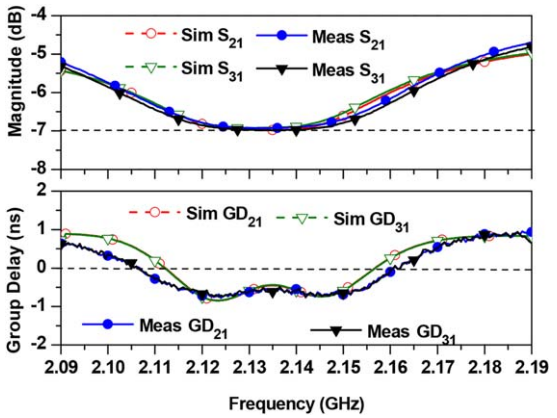

Figure 8 Simulated and measured magnitudes and GDs of the proposed power divider. [Color figure can be viewed at wileyonlinelibrary.com]

Similarly, for an experimental demonstration, the power divider with the GD of −0.5 ns is designed and fabricated at $f_0 = 2.14$ GHz. The EM-simulation layout of power divider with physical dimensions is shown in Figure 7. A $\lambda/4$ impedance transformer is used to match an input port.

The simulated and measured GDs and magnitudes of power divider are shown in Figure 8. From the measurement, the insertion losses are $|S_{21}| = -6.95$ dB and $|S_{31}| = -6.97$ dB, while the GDs are $\tau_{21} = -0.54$ ns and $\tau_{31} = -0.56$ ns at $f_0 = 2.138$ GHz. Due to the trade-off between maximum achievable NGD, insertion loss, and BW, the appropriate parameter to compare performances of circuits is an NGD-BW product. Therefore, the NGD-BW products for the different transmission paths are determined as 0.034 and 0.0336, respectively.

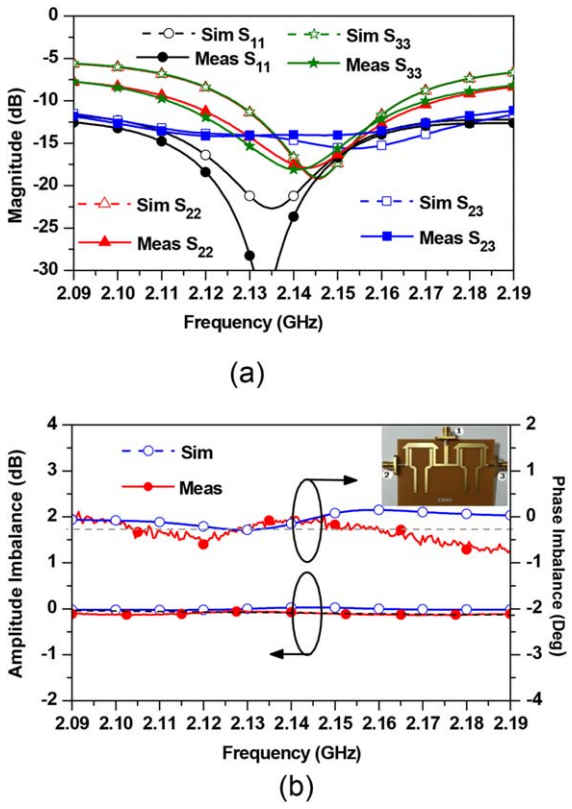

Figure 9 Simulated and measurement results of the proposed power divider: (a) return losses/isolation and (b) amplitude/phase imbalances. [Color figure can be viewed at wileyonlinelibrary.com]

The simulated and measured return losses and isolation characteristics of the power divider are shown in Figure 9(a). From the experiment, the return losses are determined as $|S_{11}| = -28.9$ dB, $|S_{22}| = -17.5$ dB, and $|S_{33}| = -18.2$ dB at f_0. The measured isolation ($|S_{23}|$) at f_0 is −15.8 dB. The measured amplitude imbalance and phase differences between the two output ports are shown in Figure 9(b). It can be seen that the maximum amplitude imbalance of ±0.1 dB and the phase imbalance of ±0.6° are observed over the bandwidth of 100 MHz.

4. CONCLUSION

In this paper, a novel method to design NGD circuit with wider bandwidth and magnitude flatness is presented based on finite unloaded quality-factor resonators. The proposed circuit does not require a lumped element resistor to generate NGD. Analytical design equations are provided to calculate the coupling matrix with predefined NGD. The proposed circuit topology was further apply to design power divider with predefined NGDs. The design theory was validated through fabrication of NGD circuit and power divider at center frequency of 2.14 GHz. The proposed circuit can be applied in various applications of communication systems.

ACKNOWLEDGMENT

This work was supported by the Basic Science Research Program through the National Research Foundation of Korea (NRF) funded by the Ministry of Education, Science and Technology 2016R1D1A1A09918818.

REFERENCES

1. C.H. Hymel, M.H. Skolnick, R.A. Stubbers, and M.E. Brandt, Temporally advanced signal detection: A review of technology and potential applications, IEEE Circuit Syst Mag 11 (2010), 10–25.
2. L. Brillouin and A. Sommerfeld, Wave propagation and group velocity (1960), pp. 113–137.
3. H. Choi, Y. Jeong, C.D. Kim, and J.S. Kenney, Efficiency enhancement of feedforward amplifiers by employing a negative group delay circuit, IEEE Trans Microw Theory Tech 58 (2010), 1116–1125.
4. B. Ravelo, M.L. Roy, and A. Perennec, Application of negative group delay active circuits to the design of broadband and constant phase shifters, Microw Opt Technol Lett 50 (2008), 3078–3080.
5. S. Lucyszyn and I. D. Robertson, Analog reflection topology building blocks for adaptive microwave signal processing applications, IEEE Trans Microw Theory Tech 43 (1995), 601–611.
6. H. Mirzaei and G.V. Eleftheriades, Realizing non-Foster reactive elements using negative group delay networks, IEEE Trans Microw Theory Tech 61 (2013), 4322–4332.
7. G. Chaudhary and Y. Jeong, A design of compact wideband negative group delay network using cross coupling, Microw Opt Technol Lett 56 (2014), 2495–2497.
8. G. Chaudhary and Y. Jeong, Microstrip line negative group delay filters for microwave circuits, IEEE Trans Microw Theory Tech 62 (2014), 234–243.
9. C.T.M. Wu and T. Itoh, Maximally flat negative group delay circuit: A microwave transversal filter approach, IEEE Trans Microw Theory Tech 62 (2014), 1330–1342.
10. J. Yi, Y. Yang, M. Park, W. Kang, and B. Kim, Analog predistortion linearizer for high power RF amplifiers, IEEE Trans Microw Theory Tech 48 (2000), 2709–2913.
11. J.S. Hong and M.J. Lancaster, Microstrip filters for RF/microwave applications, John Wiley & Sons Inc., New York, NY, 2001, pp. 19–21.
12. H.R. Ahn, Asymmetric passive components in Microwave Integrated Circuits, Wiley, Hoboken, NJ, 2006.